Particle-in-Cell simulations for laser –plasma interactions

Tatsufumi Nakamura

Japan Atomic Energy Agency (JAEA)
8-1-7 Umemidai, Kizugawa, Kyoto 619-0215, JAPAN

Contents

References

"Plasma Physics via Computer Simulation", McGraw-Hill (New York), by C.K.Birdsall and A.B.Langdon.

"Computational Plasma Physics : With Applications to Fusion and Astrophysics", Addison-Wesley, by T.Tajima.

"Computer Simulation Using Particles", McGraw-Hill (New York), by R.W.Hockney and J.W.Eastwood.

Particle-in-Cell simulation

Particle-in-Cell (PIC) method

- Temporal evolution of plasma is simulated.
  many body system with electromagnetic interaction

- Kinetic description is used (c.f. fluid description).
  wave-breaking, particle trapping, etc.

- Spatial grid is introduced for EM field (c.f. direct potential calculation as MD)
  spatial smoothing, no need to storage particle trajectories (x,v)

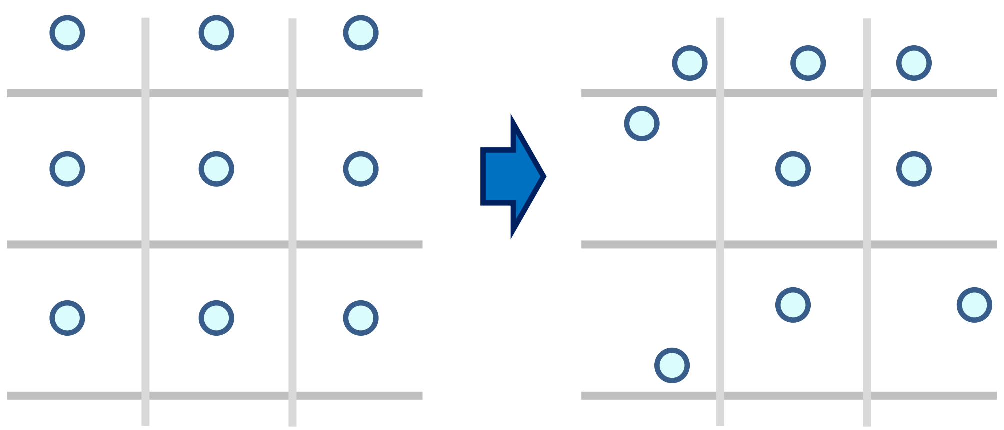

Particles and fields in PIC

Time evolution of particles and fields are calculated self-consistently.

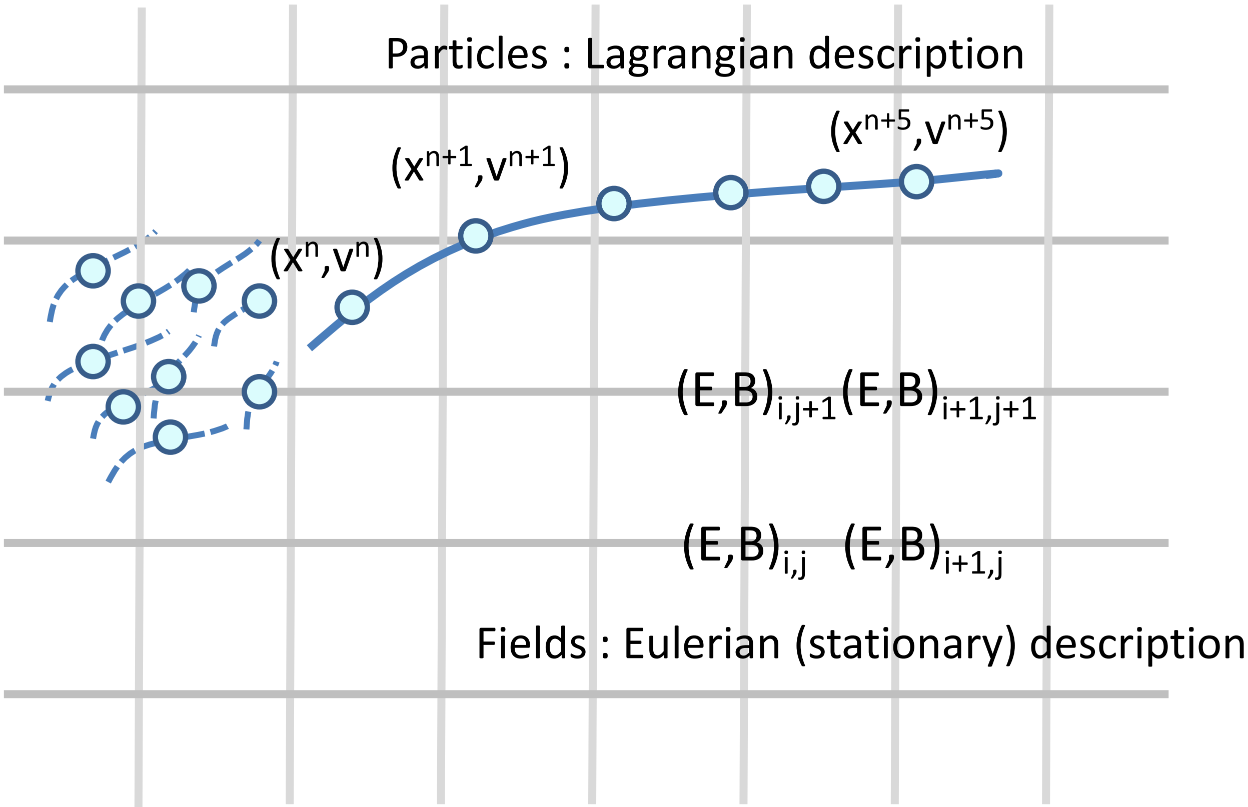

Particles and fields are treated using different descriptions.

One cycle for time evolution in PIC

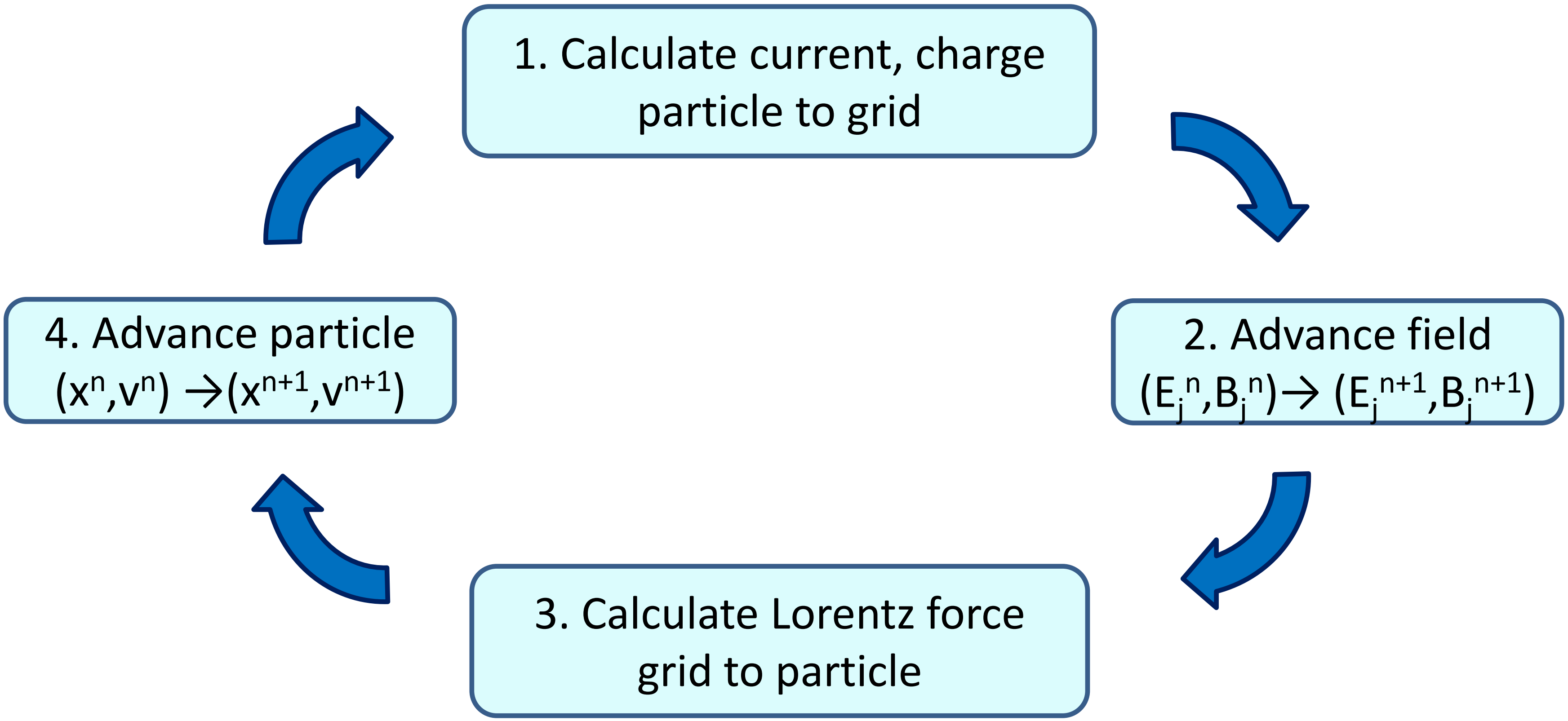

1. Calculate current and charge density : particle to grid

Current and charge densities are calculated by summing all particle's contribution to each grids.

$$J_j = \sum_i J_{j,i}$$

$$\rho_j = \sum_i \rho_{j,i}$$

Area weighting for 1D case

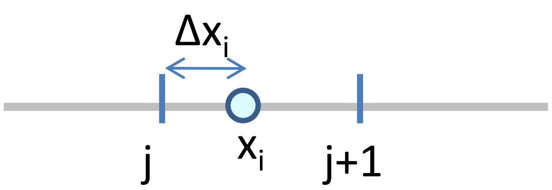

j,j+1 : grid position

x_i : position of i-th particle

$\Delta x_i = x_i - \lfloor x_i \rfloor$

Linear weighting

$$\rho_{j,i} = q_i(1-\Delta x_i)$$

$$\rho_{j+1,i} = q_i(\Delta x_i)$$

multiple v_i for current density.

Higher order weighting

$$\rho_{j-1,i} = q_i \frac{1}{2}(\frac{1}{2} - \Delta x_i)^2$$

$$\rho_{j,i} = q_i(\frac{3}{4} - \Delta x_i^{\ 2})$$

$$\rho_{j+1,i} = q_i \frac{1}{2}(\frac{1}{2} + \Delta x_i)^2$$

2. Advance fields : solving Maxwell's equations

Electric and magnetic fields are calculated from Maxwell's equations.

$$\frac{\partial \vec{E}}{\partial t} = c^2 \nabla \times \vec{B} - \frac{\vec{J}}{\varepsilon_0}$$

$$\frac{\partial \vec{B}}{\partial t} = -\nabla \times \vec{E}$$

Time evolution of E,B is calculated.
Particle-Field coupling is calculated through J.

$$\nabla \cdot \vec{B} = 0$$

$$\nabla \cdot \vec{E} = \frac{\rho}{\varepsilon_0}$$

Independent on time.
To be satisfied at initial condition.

2. Advance fields : solving Maxwell's equations

In 2D case, equations for E-field is written as

$$Ex_{i,j}^{n+1} = Ex_{i,j}^{n} + Bz_{i,j}^{n+1/2} - Bz_{i,j-1}^{n+1/2} - Jx_{i,j}^{n+1/2}$$
$$Ey_{i,j}^{n+1} = Ey_{i,j}^{n} - Bz_{i,j}^{n+1/2} + Bz_{i,j-1}^{n+1/2} - Jy_{i,j}^{n+1/2}$$
$$Bz_{i,j}^{n+1} = Bz_{i,j}^{n} + Ey_{i,j}^{n+1/2} - Ey_{i-1,j}^{n+1/2} - Ex_{i,j}^{n+1/2} + Ex_{i,j-1}^{n+1/2}$$

Centered spatial and time difference assures second order accuracy.

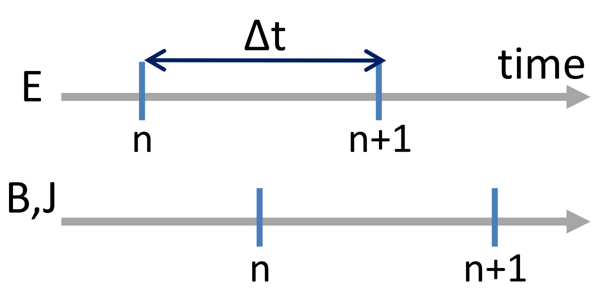

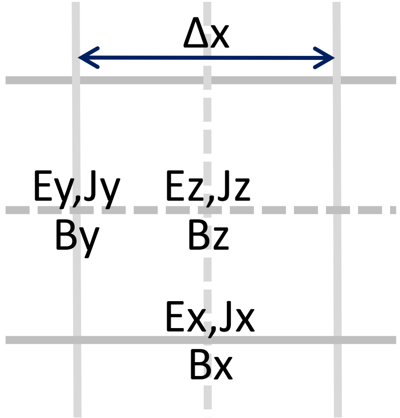

Correction to satisfy charge conservation

Due to the inconsistency of current and charge densities, Gauss's law is not satisfied.

$$\nabla \cdot \vec{E} \neq \frac{\rho}{\varepsilon_0}$$

We need to obtain correct electric field corresponding to the charge density.

$$\nabla \cdot \vec{E}' = \frac{\rho}{\varepsilon_0}$$

The correction $\vec{E}' - \vec{E} = -\nabla \delta\phi$ is calculated from

$$\nabla^2 \delta\phi = \nabla \cdot \vec{E} - \frac{\rho}{\varepsilon_0}$$

Charge conservation scheme

The scheme to achieve charge conservation is proposed.
T.Esirkepov, Comput. Phys. Comm. 135, 144 (2001).

Calculate current density to exactly satisfy the charge conservation law.

$$(\rho_j^{n+1} - \rho_j^n) + (J_j^{n+1/2} - J_{j-1}^{n+1/2}) = 0$$

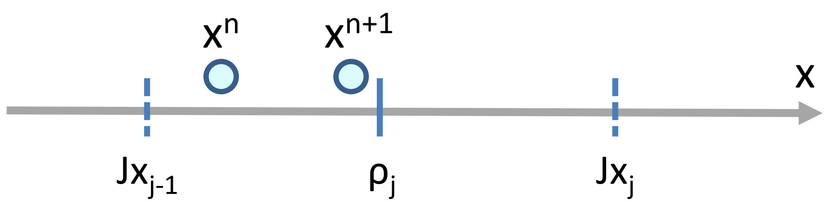

Movement of i-th charged particle $x_i^n \rightarrow x_i^{n+1}$, changes the charge density at x=i.
The time-difference of ρ_{ji} should be the difference between $Jx_{j-1,i}$ and $Jx_{j-1,i}$.

When i-th particle moves in j-1<x<j, $(\rho_{j-1,i}{}^n , \rho_{j,i}{}^n) \rightarrow (\rho_{j-1,i}{}^{n+1} , \rho_{j,i}{}^{n+1})$.
This leads to $Jx_{j-2,i}=0$, $Jx_{j-1,i}=-\rho_{j-1,i}{}^{n+1}+\rho_{j-1,i}{}^n$ and $Jx_{j,i}=Jx_{j-1,i}-\rho_{j,i}{}^{n+1}+\rho_{j,i}{}^n$.

3. Calculate Lorentz force : grid to particle

In calculating the Lorentz force, electric and magnetic field at each particle positions should be calculated.

Area weighting for 1D case

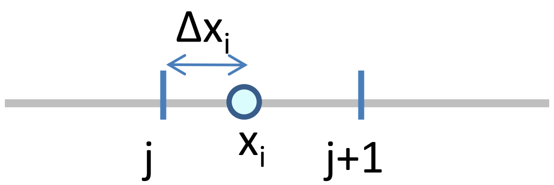

j,j+1 : grid position
x_i : position of i-th particle
$\Delta x_i = x_i - |x_i|$

Linear weighting

$$Ex = Ex_j (1 - \Delta x_i) + Ex_{j+1} \Delta x_i$$

Higher-order weighting

$$Ex = Ex_{j-1} \frac{1}{2} (\frac{1}{2} - \Delta x_i)^2 + Ex_j (\frac{3}{4} - \Delta x_i^{\ 2}) + Ex_{j+1} \frac{1}{2} (\frac{1}{2} + \Delta x_i)^2$$

Magnetic field is advanced for half-time step to coincide with electric field.

4. Advance particle : solving Newton-Lorentz equation

Particle position and momentum are advanced from the following equations;

$$\vec{p}^{\,n+1/2} - \vec{p}^{\,n-1/2} = q_i \left(\vec{E}^n + \frac{\vec{p}_i^{\,n+1/2} + \vec{p}_i^{\,n-1/2}}{2m\bar{\gamma}} \times \vec{B}^n \right),$$

$$\vec{x}^{\,n+1} - \vec{x}^{\,n} = \frac{\vec{p}^{\,n+1/2}}{m\gamma^{n+1/2}}.$$

Newton-Lorentz equation is solved by using Boris's method.

$$\begin{cases} \vec{p}^{\,n-1/2} = \vec{p}^{\,-} - q_i \vec{E}^n / 2 \\ \vec{p}^{\,n+1/2} = \vec{p}^{\,+} + q_i \vec{E}^n / 2 \end{cases} \Rightarrow \quad \vec{p}^{\,+} - \vec{p}^{\,-} = \frac{q_i}{2m\bar{\gamma}} (\vec{p}^{\,+} + \vec{p}^{\,-}) \times \vec{B}$$

rotation from p^- to p^+

$$\tan\frac{\theta}{2} = \frac{|\vec{p}^{\,+} - \vec{p}^{\,-}|}{|\vec{p}^{\,+} + \vec{p}^{\,-}|}$$

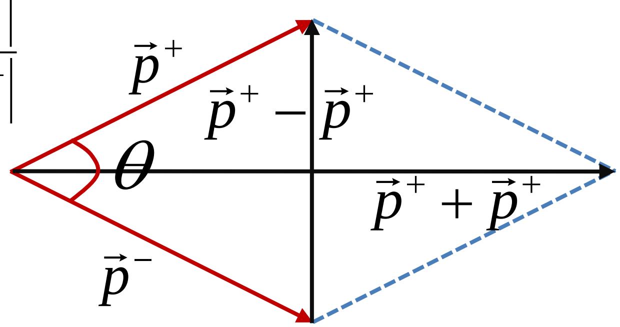

1. Calculate p^-
2. Rotate to p^+
3. Calculate $p^{n+1/2}$

Time flow of PIC method

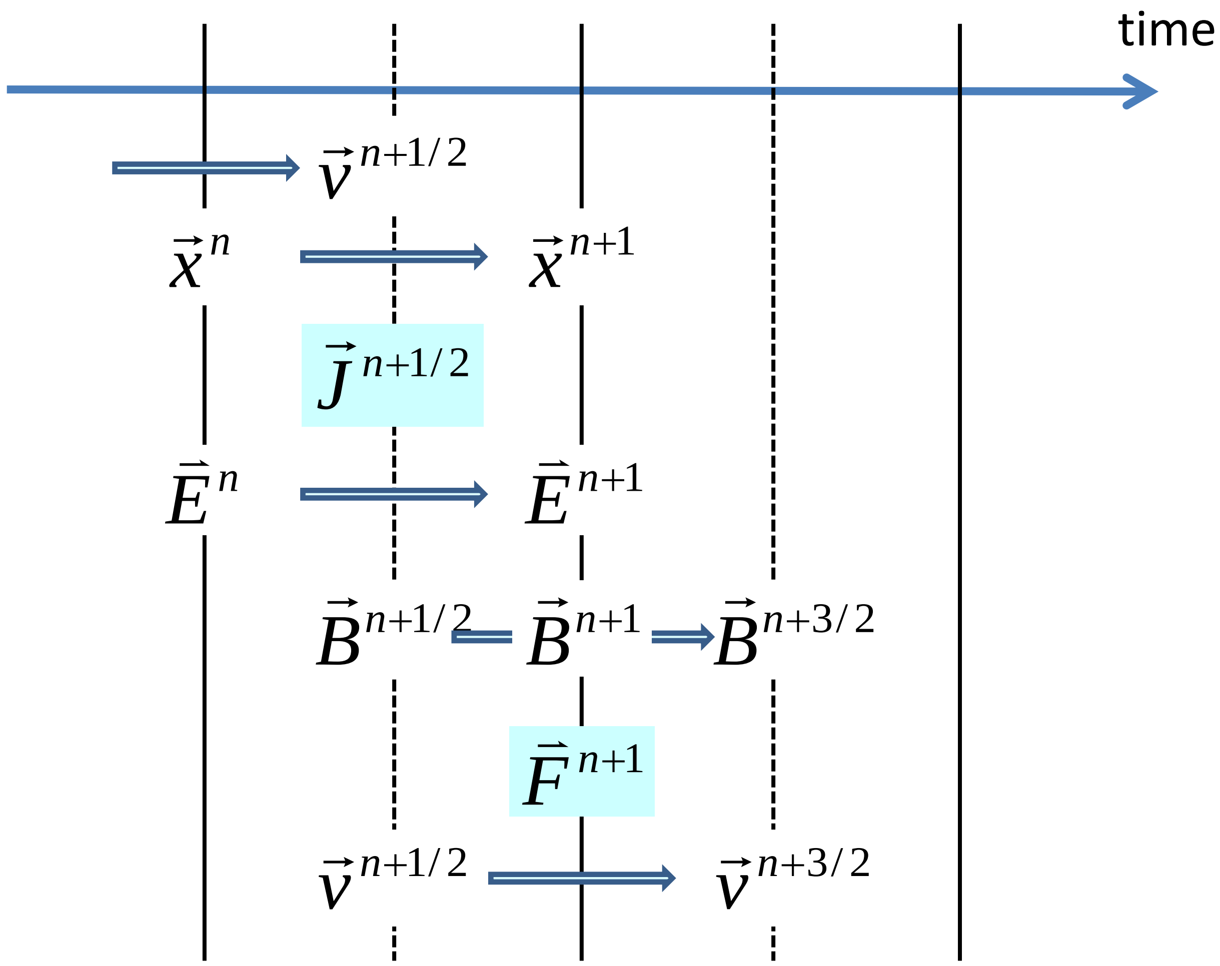

Ionization process in PIC

By including ionization process in PIC, plasma non-uniformity of fast time scale is analyzed.

- Laser spectral blue-shift
- Laser modulation
- Ionization injection for LWFA
- High contrast laser interaction with matter

Procedures of ionization process in PIC

1. Calculate ionization rate
2. Judge ionization process to occur (Monte Carlo)
3. Add new-born electron
4. Add charge state of ion/atom by one
5. Correction on current density to satisfy energy balance, $\vec{J} \cdot \vec{E} \Delta t = I_{ion}$

Field ionization

Ionization rate of optical field ionization   L.Keldysh, Sov. Phys. JETP 20, 1307 (1965)

$$\nu(E) = \frac{4me^4}{\hbar^3}\left(\frac{I_{ion}}{I_h}\right)^{2/5}\frac{E_a}{E}\exp\left(-\frac{2}{3}\left(\frac{I_{ion}}{I_h}\right)^{3/2}\frac{E_a}{E}\right)$$

I_{ion}: ionization potential. I_h: ionization potential for hydrogen.

E_a : E-field at Bohr radius.

Ionization rate for He

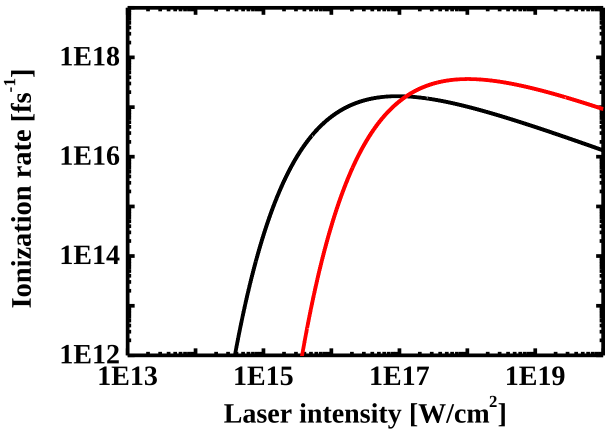

Ionization rate for C

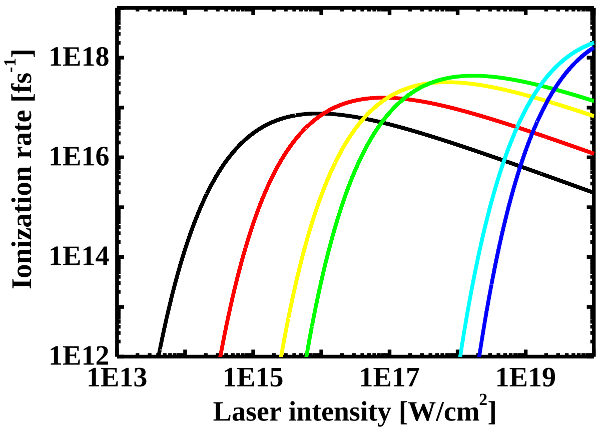

Collisional ionization

Cross section for collisional ionization (BEB model)   Y.Kim etal., PRA 50, 3549 (1994)

$$\sigma(t) = \frac{4\pi r_B^2 N E_R^2}{(1+K)} \left\{ \left(\frac{1}{2} - \frac{1}{2K^2} \right) \ln K + (1 - \frac{1}{K}) - \frac{\ln K}{1+k} \right\}$$

r_B Bohr radius N Electron number in subshell

E_R Rydberg energy K Incident energy/binding energy

Comparison with experiments

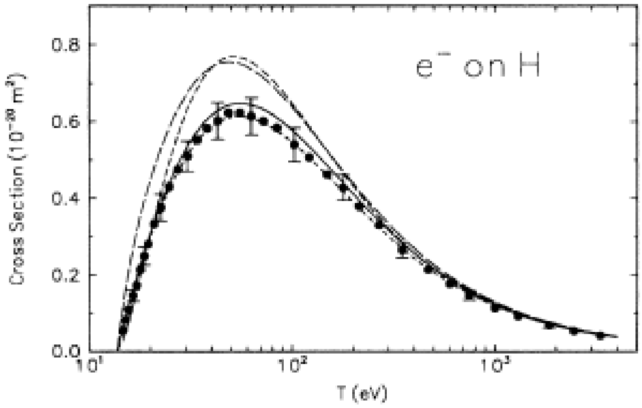

Laser blue-shift via ionization

Laser pulse propagating through gas target ionizes it simultaneously.
A density down ramp is induced at the front of laser pulse, which leads to spectral blue-shift.

E.Esarey etal., PRE 44, 3908 (1991)
W.Wood etal., PRL 67, 3523 (1991)
J.Koga etal., PoP 7, 5223 (2000)

$$\Delta\omega = -\frac{\omega_0}{c}\int_0^z \frac{\partial n(t)}{\partial t}\,dt$$

Experiments

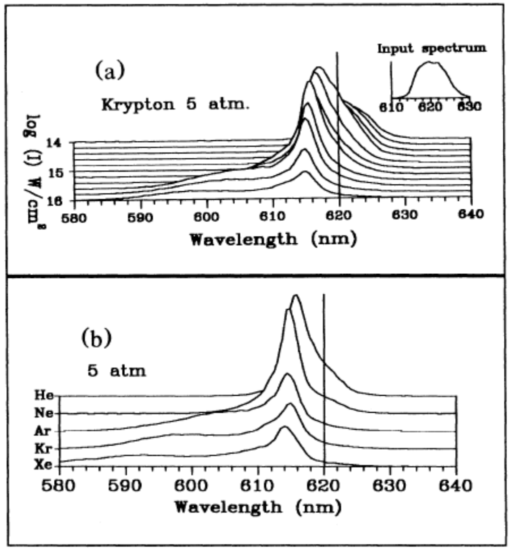

Simulation

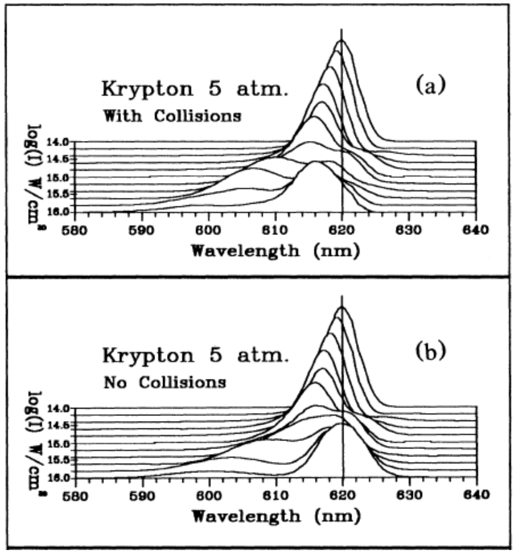

Laser modulation due to ionization

Laser pulse propagating through gas target ionizes it simultaneously. Ionization leads to plasma density inhomogeneity in transverse to the wave vector, which leads to laser diffraction.

P.Sprangle etal., PRE 54, 4211 (1996)

Laser propagation in nitrogen gas

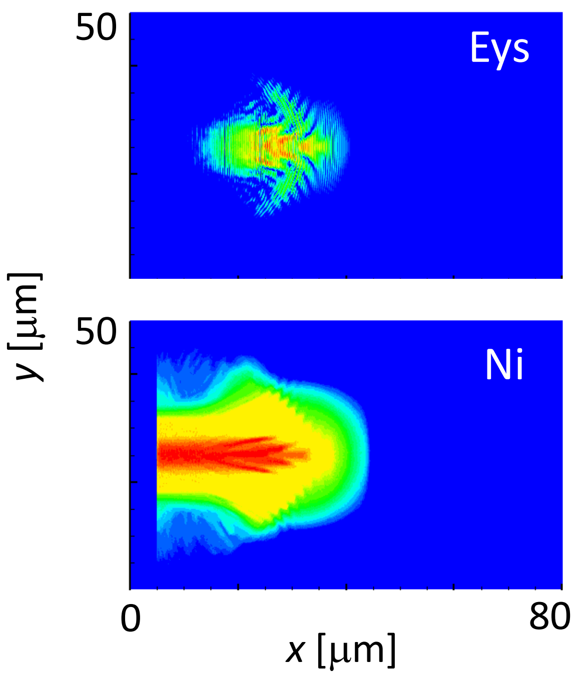

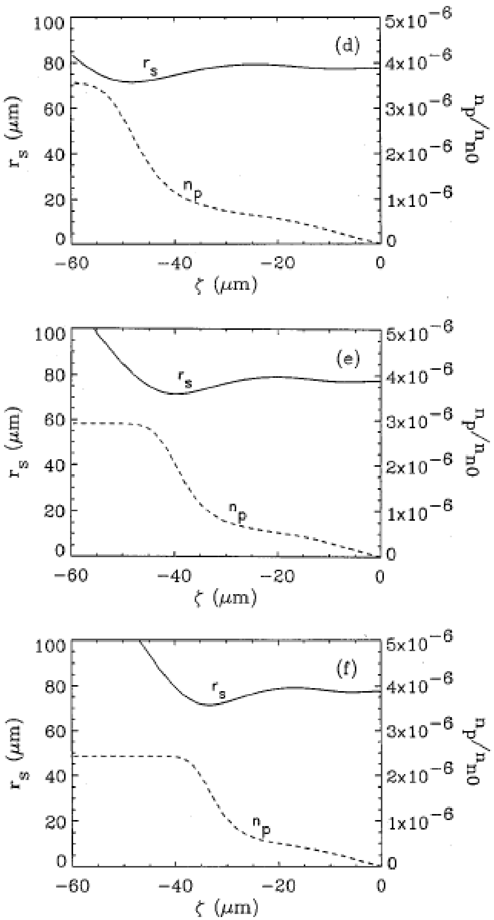

Electron injection due to ionization

Laser pulse propagating through gas target ionizes it simultaneously.
Ionization generates new-born electrons inside the wake potential.

E.Oz etal., PRL 98, 084801 (2007)
A.Pak etal., PRL 104, 025003 (2010)

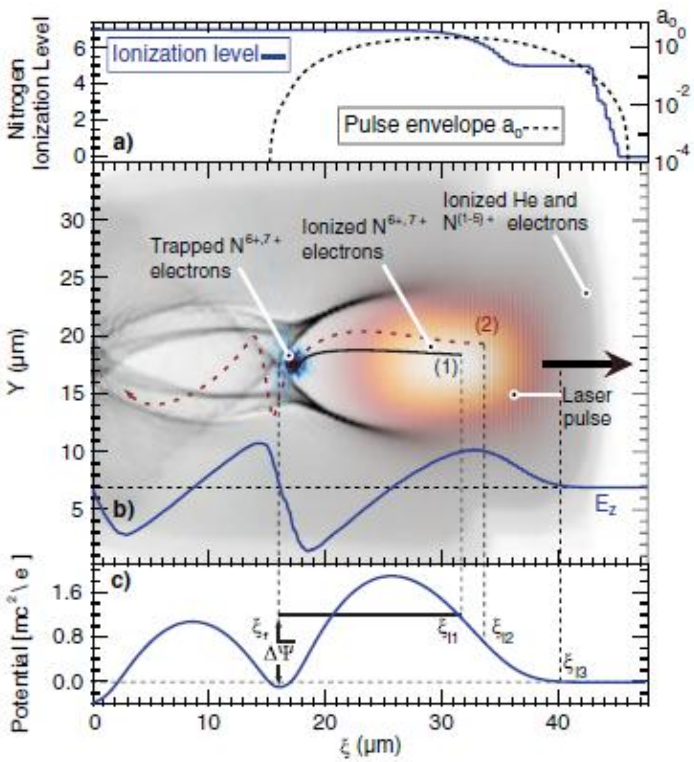

High contrast laser and form interaction

High contrast laser pulses are used to increase laser-plasma coupling.
This involves electron acceleration and generation.

T.Nakamura, PoP 17, 113107 (2010)

SiO_2 foam manufactured at Osaka U.

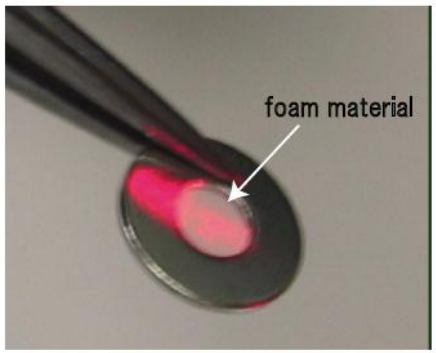

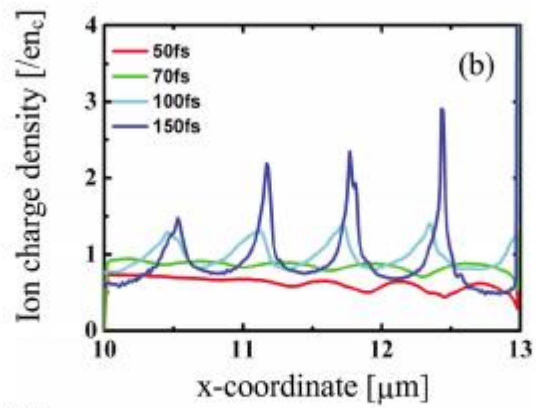

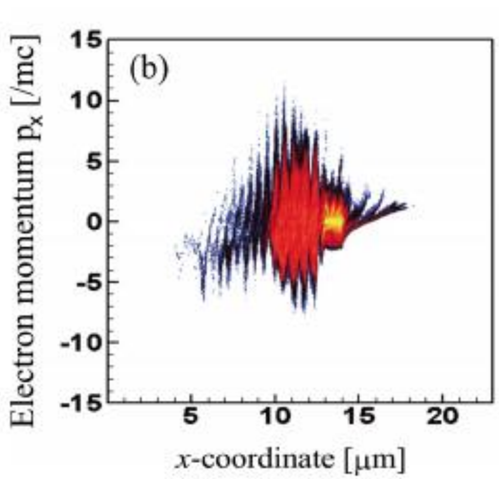

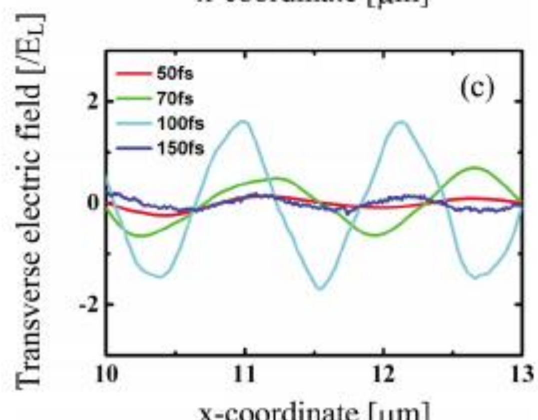

- Photo ionization process

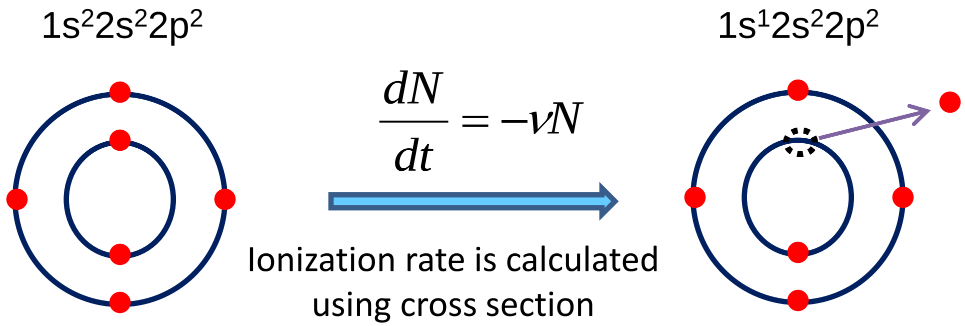

$$\frac{dN}{dt} = -\nu N$$

Ionization rate is calculated using cross section

X-ray propagation is not solved in PIC, which is modeled with photo-ionization events generating a free electron and excited atom.

- Auger process

K-shell vacancy is re-occupied by de-excitation after a certain time interval (~10fs).

These process are taken into account by introducing an electronic state for each atoms/ions.

Inner-shell and Auger ionization in PIC

Decay time of auger process for C

No.	Transition	E_{av} (eV)	A_{rav} (s^{-1})
(a)			
1	$1s2s^22p^2$–$1s^22s^22p$	287	2.69×10^{11}
2	$1s2s^22p$–$1s^22s^2$	292	3.29×10^{11}
3	$1s2s2p^2$–$1s^22s2p$	292	3.22×10^{11}
4	$1s2s2p$–$1s^22s$	298	2.61×10^{11}
5	$1s2p^2$–$1s^22p$	298	3.85×10^{11}
6	$1s2p$–$1s^2$	305	4.67×10^{11}
7	$2s^22p^2$ –$1s2s^22p$	347	1.05×10^{12}
8	$2s^22p$–$1s2s^2$	352	6.09×10^{11}
9	$2s2p^2$–$1s2s2p$	352	1.21×10^{12}
10	$2s2p$–$1s2s$	358	7.00×10^{11}
11	$2p^2$–$1s2p$	358	1.40×10^{12}
12	$2p$–$1s$	357	8.13×10^{11}

K.Moribayashi, J.Phys.B 41, 1 (2008)

Cross section of photo-ionization for C

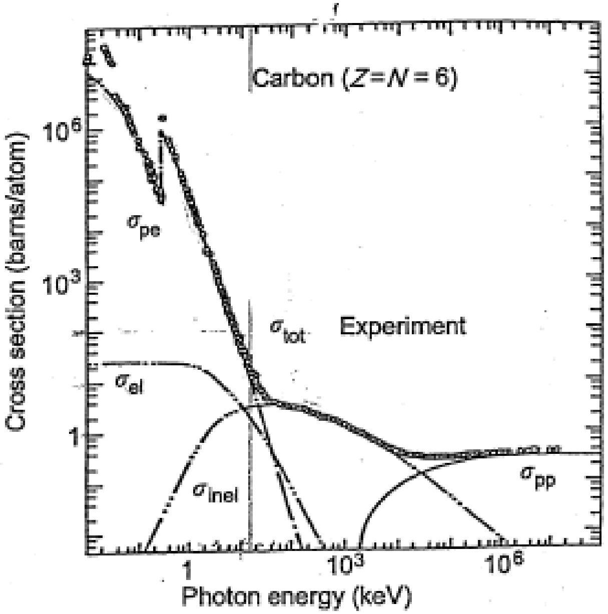

H.Gerstenberg etal., Nucl. data sci. tech (1982)

Interaction of XFEL light with cluster target
(modeling bio-molecule)

Irradiation of intense X-ray onto bio-molecule

1. **Photo-ionization process**
   Inner shell ionization is dominant in photo-ionization (12keV).
   Electrons with energy~12 keV are generated.

2. **Relaxation by Auger effect, Coulomb collision**
   Auger ionization generates additional free electron~ 100 eV.
   Further ionization takes place via collisional ionization.

3. **Plasma dynamics**
   Strong sheath field is induced by 12 keV electrons which quickly ionizes targets via field ionization.
   Field ionization is not considered so far in XFEL-matter interaction.

MD simulation

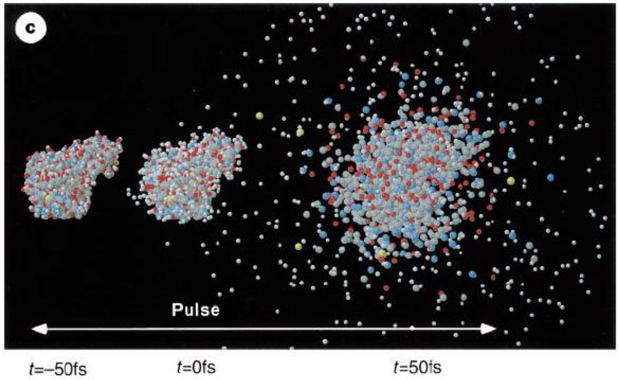

R.Neutze, et al., Nature 406, 752 (2000)

Simulation methods for XFEL-matter interaction

Numerical approaches on interaction of XFEL light with targets

1. Quantum – classical method : cross section + rate equation

   e.g., S.Hau-Reige, et al., PRA 69, 051906 (2004)

   - Easy for parameter survey.
   - No spatial information. Additional modeling is needed to calculate collisional ionization (electron trapping), field ionization.

2. Molecular Dynamics simulation for protein structure (GROMACS etc.)

   e.g., R.Neutze, et al., Nature 406, 752 (2000)

   - Information of target configuration (protein structure).
   - Neglecting high energy electron motion. Field ionization is not taken into account.

3. Particle-in-Cell simulation
   - Plasma dynamics is treated, which plays a key role when the density of high energy (12 keV) electrons becomes high.
   - Target configuration is not treated.

Evaluation of sample damage by X-ray irradiation

T.Nakamura, Y.Fukuda, Y.Kishimoto,
PRA 80, 053202 (2009)

Average number of bound electrons

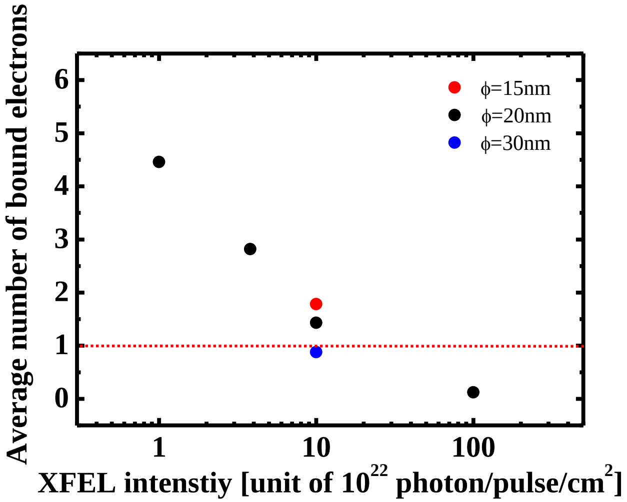

Time-average of number of bound electrons is defined as,

$$\left\langle \overline{Ne} \right\rangle = \frac{\int \langle Ne(t) \rangle I(t)dt}{\int I(t)dt},$$

, where $\langle Ne(t) \rangle$ represents ensemble-averaged bound electron number per atom. Intensity of $>10^{23}$ photon/pulse/cm^2 leads to generation of fully ionized atoms.

High energy ion generation via magnetic vortex acceleration

T.Nakamura, S.V.Bulanov, T.Zh.Esirkepov, M.Kando

Japan Atomic Energy Agency (JAEA)
8-1-7 Umemidai, Kizugawa, Kyoto 619-0215, JAPAN

Contents

Applications of laser-accelerated ions

Laser-accelerated ion source

- Medical application
  T.Tajima, J. Jpn. Soc. Therap. Rad. Oncol. (1998)
- Plasma diagnostics
  M.Borghesi, et al., Phys. Plasmas (2002)
- Laser fusion driver
  M.Roth, et al., Phys. Rev. Lett. (2001)

Cancer therapy by ion beam

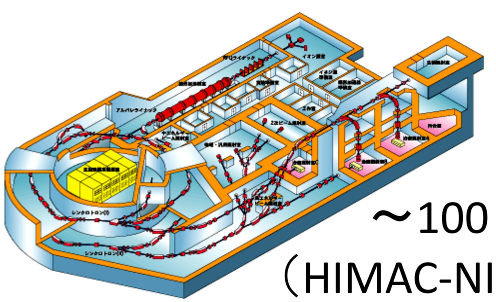

～100 m
（HIMAC-NIRS）

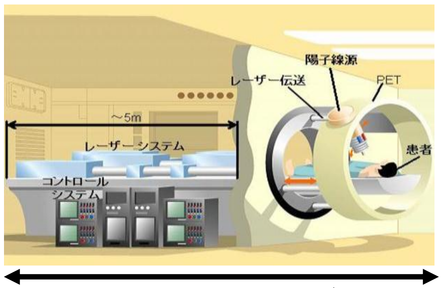

～10 m （future plan）

Laser-ion-acceleration can realize compact ion source

New acceleration scheme is needed for compact ion source

Important issue is energy enhancement.
200 MeV proton is required for medical application.

Ion acceleration by sheath field

A.V.Gurevich, et al., Sov. Phys. JETP (1966),
S.C.Wilks, et al., Phys. Plasmas (2001),
P.Mora, Phys. Rev. Lett. (2003), many others.

- Robust and established scheme
- Energy scaling predicts PW-class laser is needed for 200 MeV proton generation

M.Borghesi, et al., Fus.Sci.Tech. (2006)

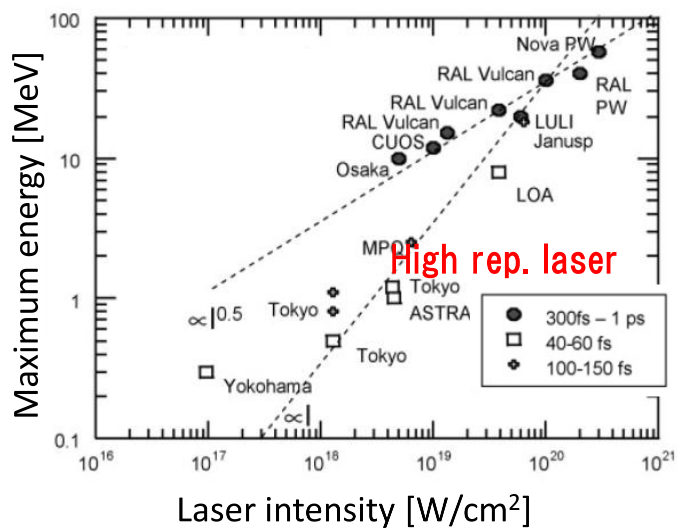

For medical applications,
we need more efficient acceleration !

New acceleration scheme is needed for ion source

Ion energy enhancement by using gas (near-critical) target

- Replenishable target, favor for high rep. operation
- Near-critical plasma realizes high energy absorption

Ion acceleration from underdense, near-critical plasmas.

L.Willingale, et al., Phys. Rev. Lett. (2006)

Y.Fukuda, et al., Phys. Rev. Lett. (2009)

Ion acceleration by magnetic vortex inside plasma

S.V.Bulanov, et al., Plasma Phys. Rep. (2005)

Energy scaling ?
Possibility for 200 MeV??

Magnetic vortex formation and ion acceleration

Laser power	100TW
Focal spot	2μm
Pulse duration	30fs
Plasma density	0.25～2Nc

Proton energy 175 MeV

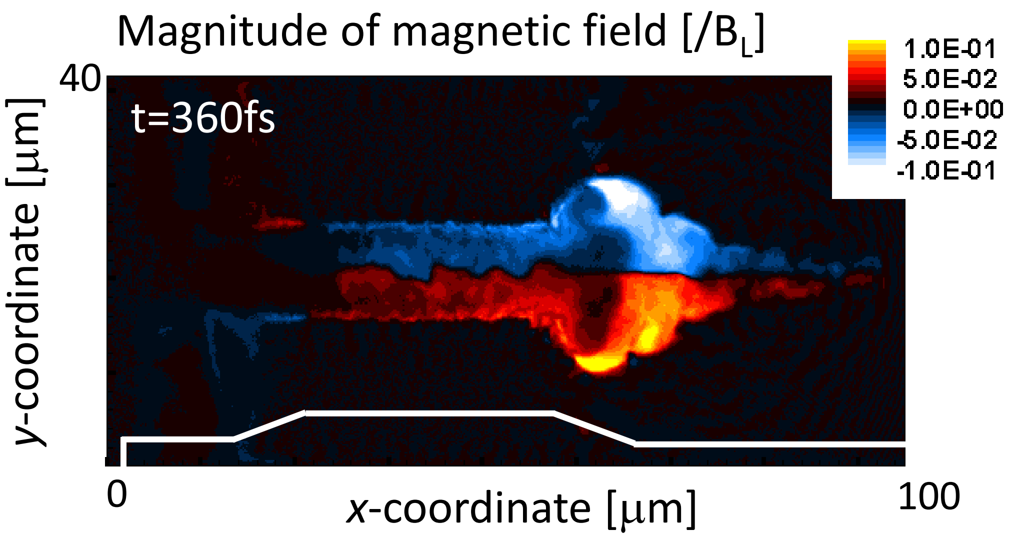

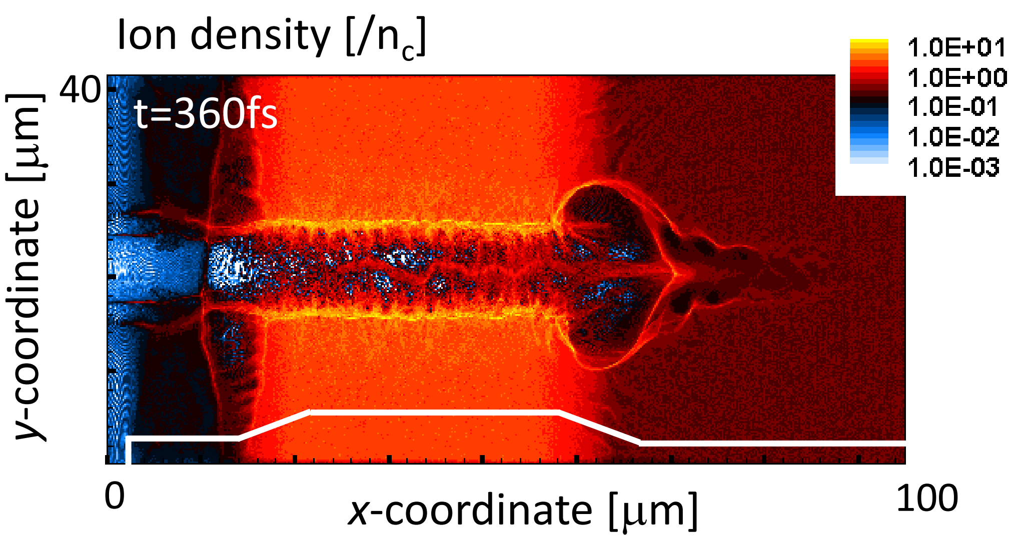

Mechanism of magnetic vortex acceleration

I

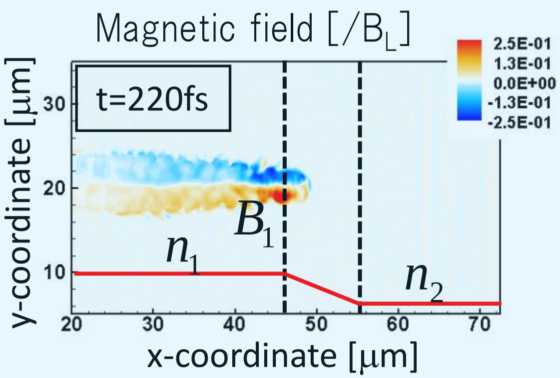

Laser propagation induces magnetic dipole vortex inside plasma.

II

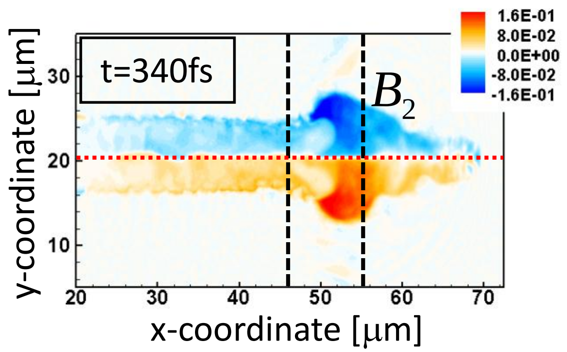

Magnetic vortex expands both in forward and lateral directions.

III

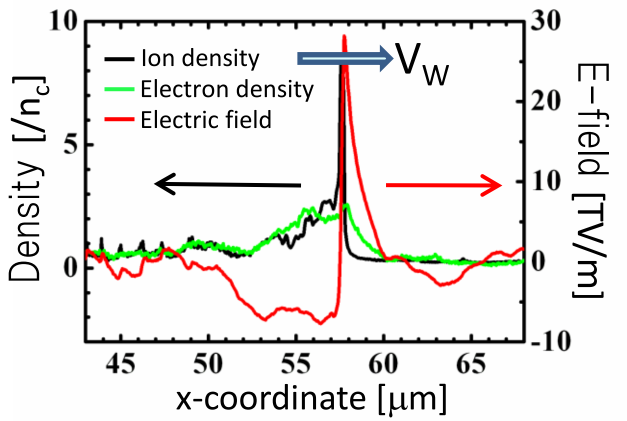

V_W : Ion wall velocity

Ions are accumulated and electric field is induced.

IV

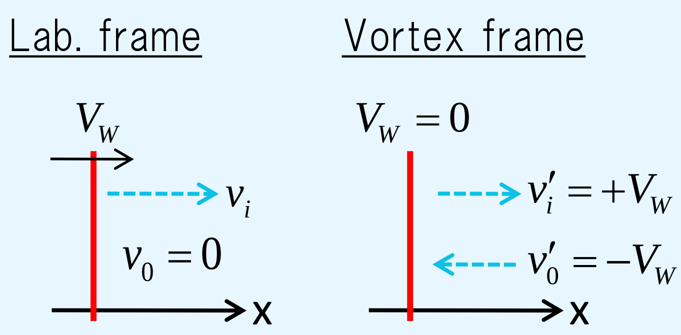

Background ions are accelerated by moving e-field.

Magnetic vortex formation in plasma

I. Magnetic dipole vortex is formed when laser energy is depleted.

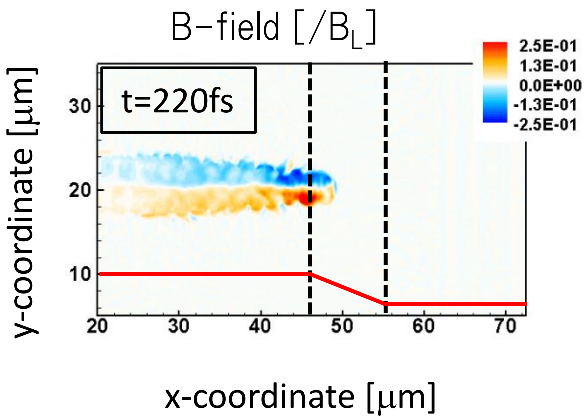

$$E(t) = N_{ph}\hbar\omega(t)$$ N_{ph} is adiabatic constant.

S.V.Bulanov, et al., Phys. Fluids B4, 1935 (1992).
W.Mori, IEEE, J. Quant. Elec. 33, 1942 (1997).

The transverse size of magnetic vortex is

$$\ell_{s1} = \frac{c\sqrt{\gamma_e}}{\omega_{p1}}, \omega_{p1} = \sqrt{\frac{n_1 e^2}{m\varepsilon_0}}, \gamma_e = \sqrt{1 + a^2/2}$$

The magnetic field of vortex is evaluated as

$$B_1 = -\mu_0 e n_1 c \ell_{s1} = -\mu_0 e n_1 c^2 \frac{\sqrt{\gamma}}{\omega_{p1}} \qquad (1)$$

Expansion of magnetic vortex at density ramp

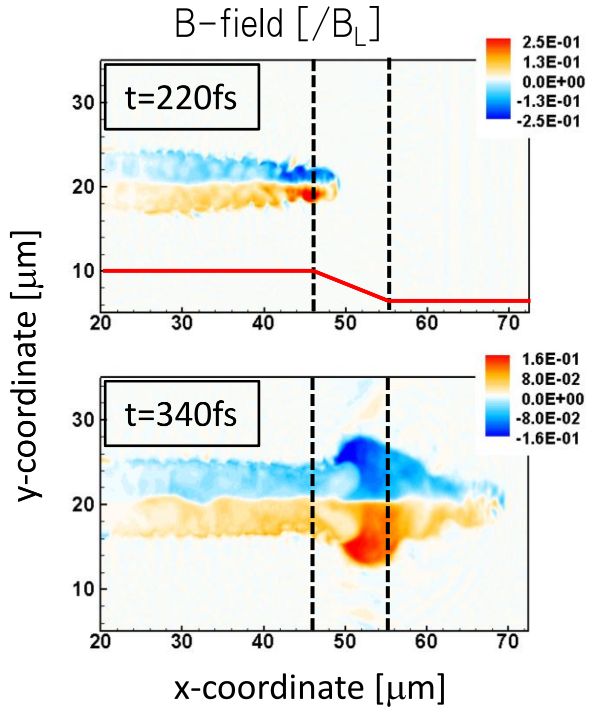

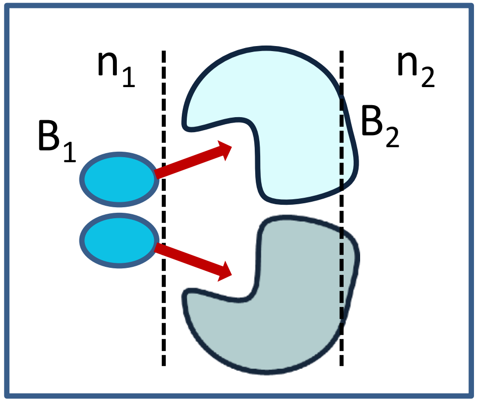

II. Vortex expands at density ramp, decreasing intensity to B_2.

$$\frac{\partial}{\partial t}\mathbf{p}+\mathbf{v}\cdot\nabla\mathbf{p}=-e(\mathbf{E}+\mathbf{v}\times\mathbf{B})-\frac{\nabla p}{n}$$

$$\frac{\partial n}{\partial t}+\nabla\cdot(n\mathbf{v})=0$$

$$p=p(n)$$

Ertel's theorem

$$\frac{d}{dt}\left(\frac{\mathbf{\Omega}}{n}\right)=\left(\frac{\mathbf{\Omega}}{n}\right)\cdot\nabla\mathbf{v},\quad \mathbf{\Omega}=\nabla\times(\mathbf{p}-e\mathbf{A})$$

$$\frac{B_1}{n_1}=\frac{2B_2}{n_1+n_2} \qquad (2)$$

Electric field is induced at vortex front

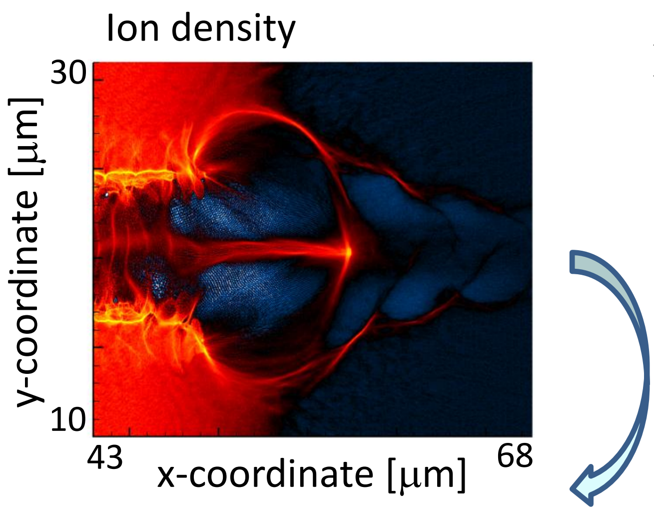

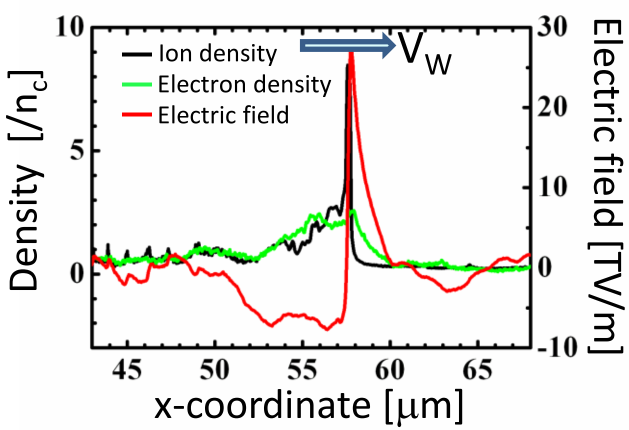

V_W : velocity of moving wall

III. Ions are accumulated and electric field is induced.

- Magnetic pressure expels electrons and ions, forming ion shell
- Electrons are circulating around vortex

➡ Electric field is induced at ion front

Ion shell moves with Alfven velocity.

$$\frac{P_W^2}{2MA} = \frac{B_2^2}{2\mu_0 n_2 / Z} \quad (3)$$

$$\frac{V_W}{c} = \frac{1}{\sqrt{1+\left(P_M / MAc\right)^2}} \frac{P_W}{MAc}$$

A : mass number
Z : ion charge

Ion acceleration by moving electric field

IV. In vortex frame, ions are reflected by electric field.

$$v_i = \frac{2V_W}{1+\beta_W^2}, \quad \beta_W = \frac{V_W}{c}$$

$$\gamma_i - 1 = \frac{2\beta_W^2}{1-\beta_W^2} = 2\left(\frac{P_M}{Mc}\right)^2$$

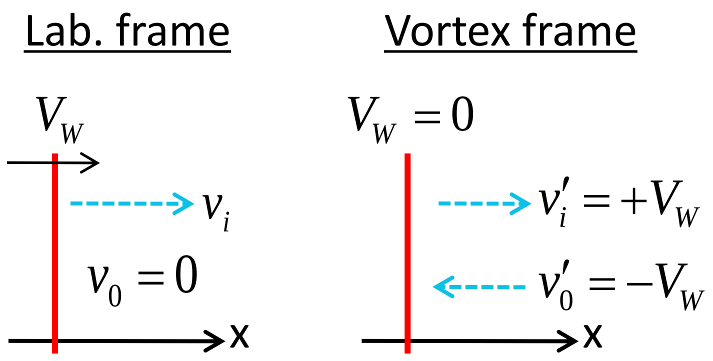

Ion maximum energy is estimated by using eqs.(1)-(3) as

$$\frac{E_i}{A} = Mc^2(\gamma_i - 1) = \left(\frac{Z}{A}\right)mc^2\frac{(n_1+n_2)^2}{2n_1n_2}\gamma_e \sim \left(\frac{Z}{A}\right)\frac{mc^2\gamma_e}{2}\frac{n_1}{n_2} \quad (n_1/n_2 >> 1)$$

Ion energy from above model is consistent with PIC results.

V_W=0.29, E=176 MeV （model）
V_W=0.28, E=175 MeV （simulation）

Energy scaling of magnetic vortex acceleration

T.Nakamura et al., PRL 105, 135002(2010).

Ion energy dependence on laser power

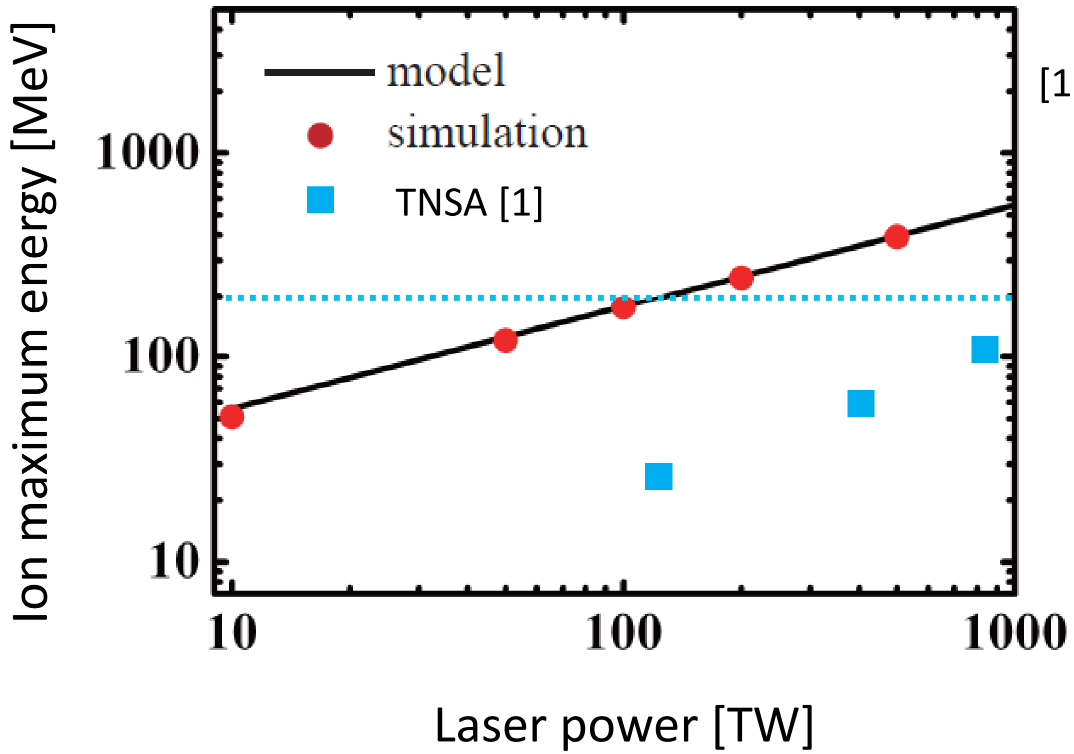

[1] PIC simulation on TNSA from J.Fuchs, et al., Nat. Phys. 2, 48 (2005).

200 MeV protons are expected to be generated by 100-class lasers.

Ions characteristics generated by magnetic vortex acceleration

Laser power	100TW
Spot size	2μm
Pulse duration	30fs

Maximum energy	175MeV	
Conversion efficiency	3.5%	
Estimated ion number	6×10^9	
Divergence angle	8 .0°	E>150MeV
	12.4°	E>100 MeV

Energy spectrum

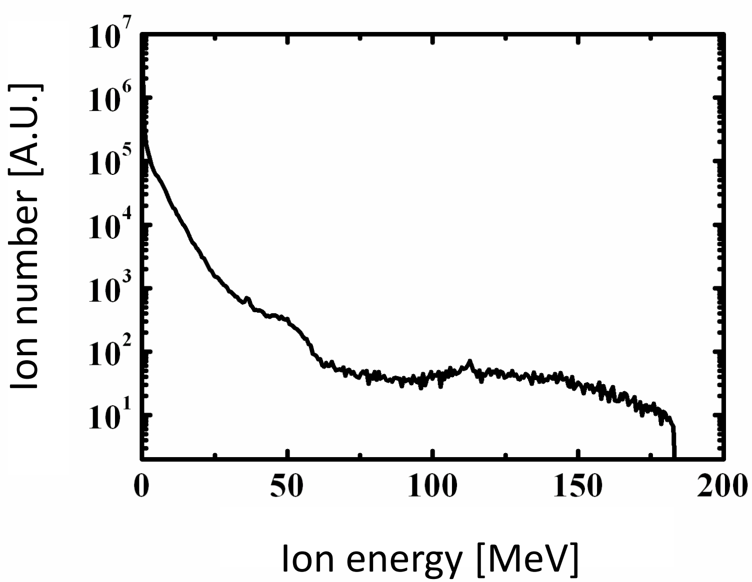

Phase plot x-px

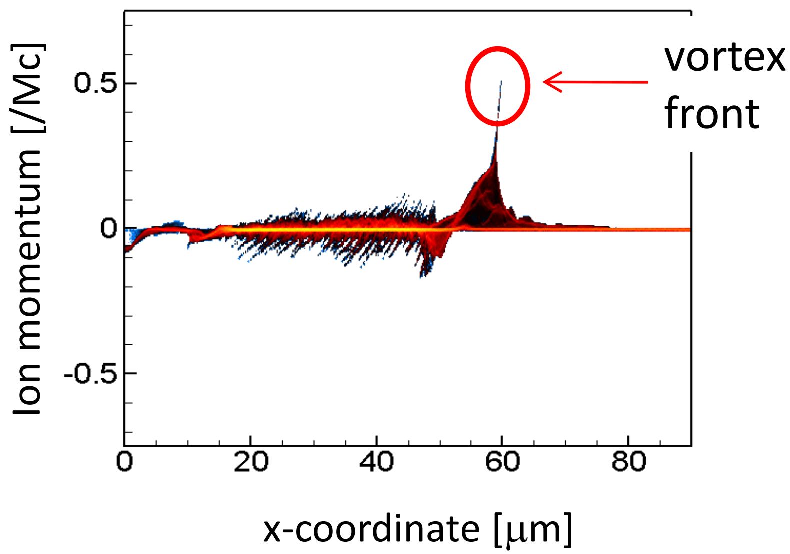

High energy ions from gas-cluster target

Y.Fukuda et al., PRL 103, 165002(2009).

Since the mixture of He and CO_2 gases are employed in the experiment, the highly charged ions of He^{n+}, C^{n+}, and O^{n+} are the possible candidates for the accelerated ions registered in the CR39 stack.

Calculation using the SRIM code

（Proton	10 MeV）	
He^{n+}	10 MeV/u	(40-MeV helium)
C^{n+}	17 MeV/u	(204-MeV carbon）
O^{n+}	20 MeV/u	(320-MeV oxygen）

- At present, we cannot tell the ion species exactly, however, two different sizes of tracks, possibly He^{n+} and C^{n+}/O^{n+}, can be recognized in the microscope images of the CR39.

Conclusions

1. We proposed magnetic vortex acceleration, which utilizes dipole vortex motion induced in near-critical density plasmas.

2. Magnetic vortex acceleration uses replenishable targets, and generates relatively high energy ions.

3. Ions generated via magnetic vortex acceleration have characteristics (energy-,angular-distributions) being favorable for laser-driven ion source.

4. The model predicts that 200 MeV proton can be generated by using 100-class laser pulse.